

Supporting Information for

Self-Assembly of Cellulose Nanofibrils by Genetically Engineered Fusion Proteins

Suvi Varjonen¹, Päivi Laaksonen¹, Arja Paananen¹, Hanna Valo², Hendrik Hähl³, Timo Laaksonen², Markus B. Linder^{1*}

¹Nanobiomaterials, VTT Technical Research Centre of Finland, Tietotie 2, P.O. Box 1000, FI-02044 VTT, Finland, ²Division of Pharmaceutical Technology, University of Helsinki, P.O. Box 56, FI-00014 University of Helsinki, Finland, ³Department of Experimental Physics, Saarland University, 66041 Saarbrücken, Germany.

LS films of proteins

Protein monolayers were studied by pipetting a known amount of HFBI and HFBI-DCBD on top of the subphase on a Langmuir trough. The films were compressed to surface pressure 30 mN/m and then picked up on a HOPG substrate. Films were then imaged by AFM (Figure S1).

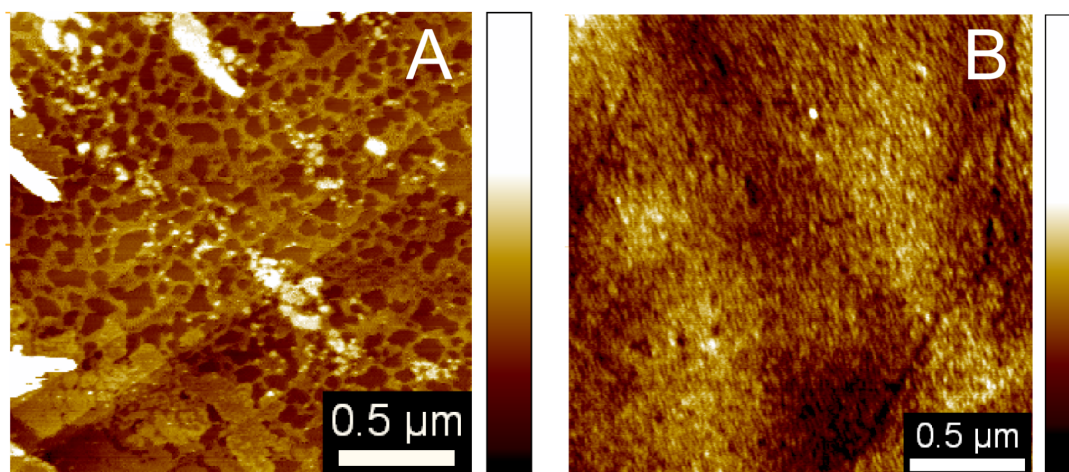


Figure S1. AFM topography images of self-assembled protein films picked up from air/water interface at surface pressure 30 mN/m. A) A monolayer of HFBI. B) A monolayer of HFBI-DCBD.

Ellipsometry

Ellipsometric measurements were carried out using a multi-wavelength ellipsometer (EP3, Nanofilm, Göttingen, Germany) operated at a single wavelength of 532 nm. The device was set up in a PCSA (polarizer-compensator-sample-analyzer) configuration with an angle of incidence of 54° to the surface normal. The air/water interface is realized by a round Teflon trough filled with buffer solution (10 mM acetate buffer, pH 5). Care was taken on choosing the optimal trough diameter, large enough to minimize meniscus curvature in the middle region, where the laser light probes the liquid/air interface. To minimize evaporation, the trough was covered by a hood with a small slit for incident and reflected light beam. The ellipsometric angles Ψ and Δ were recorded via the nulling ellipsometry principle in two zones¹ thus balancing between measurement time and accuracy of the measurement. A sampling rate of ca. 1.5 min⁻¹ was chosen for the time resolved measurements of the adsorption kinetics.

For the evaluation of the recorded data, an optical box model was applied consisting of the buffer solution (whose refractive index n_s was determined before), the protein film (assumed as homogeneous layer with a fixed refractive index n_f) and the ambient air (simulated as vacuum, $n_v = 1$). This model yields the protein layer thickness d_f as a function of time, yet with a fixed refractive index. The absolute amount of adsorbed protein Γ can be determined with de Feijter's formula

$$\Gamma = d_f \frac{n_f - n_s}{dn/dc} \quad (\text{Eq S1})$$

assuming that the refractive index of a protein is a linear function of its concentration, and with dn/dc as the increment of the refractive index due to concentration increase, fixed to a value of $0.183 \text{ cm}^3 \text{ g}^{-1}$.^{ii,iii} Since for layer thicknesses smaller than 5 nm it is not possible to determine thickness and refractive index of a layer unambiguously^{iv,i}, the adsorbed amount Γ is the more reliable value.

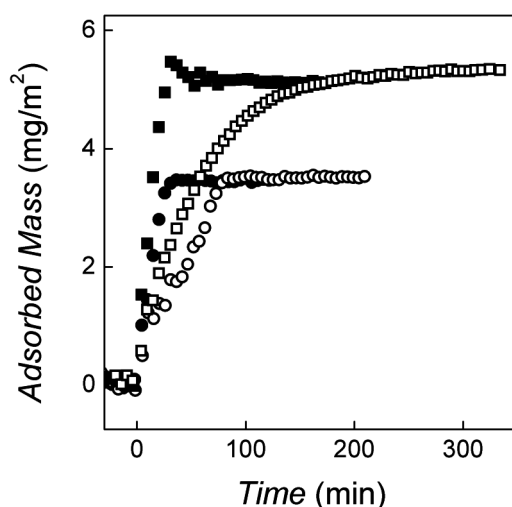


Figure S2. Adsorbed mass of HFBI (circles) and HFBI-DCBD (squares) at the air/water interface as a function of time. Closed symbols correspond to protein concentrations $1 \mu\text{M}$ and open symbols to $0.5 \mu\text{M}$.

Adsorption HFBI and HFBI-DCBD at air/water interface was studied by injecting certain amounts of the proteins into water and measuring the evolution of a surface film. After observing a constant baseline indicating constant ambient conditions, the measurements were started by exchanging 10 ml of the buffer with the protein solution. Complete mixing was achieved by injecting the protein solution into the bulk water at velocities sufficiently high for turbulent flow behavior. Measurement was repeated with protein concentrations $0.5 \mu\text{M}$ and $1.0 \mu\text{M}$ (Figure S2.). The final adsorbed masses of HFBI ($M = 7.54 \text{ kDa}$) and HFBI-DCBD (18.50 kDa) were 3.5 mg/m^2 and $\sim 5.1 \text{ mg/m}^2$, respectively. These correspond to monolayers with mean molecular areas 3.6 nm^2 and 6.0 nm^2 .

QCM Analysis of Functionality of the HFB-DCBD Fusion Protein.

Quartz Crystal Microbalance. A quartz crystal microbalance (QCM) was used for simultaneous measurement of frequency and dissipation (D4-QCM system, Q-Sense AB, Sweden) to follow the binding of CNC to a HFBI-DCBD or HFBI surface. The gold-coated quartz crystal sensor chips were spin coated with polystyrene to yield a 20 nm ($\pm 30\%$) thick hydrophobic surface as follows: First the sensor chips were cleaned in a standard UV/ozone chambers for 10 minutes and exposed to hot $\text{H}_2\text{O}/\text{NH}_3/\text{H}_2\text{O}_2$ mixture (1:1:5) for 10 minutes followed by rinsing with Milli-Q water. The dried sensor chips were placed on a spin

coater and 2 to 3 drops of 0.5 w-% polystyrene solution in toluene were placed on the sensor chip and spinned to a film. For both HFBI and HFBI-DCBD, 5 μ M protein solutions (500 μ l) were injected using a flow of 0.1 ml/min. The sensor was equilibrated until the resonance frequency (fifth overtone) was stable (30 min). The surface was then washed with buffer (50 mM sodium phosphate buffer pH 7.0) until the signal stabilized again. A 0.1 mg/ml solution of CNC in the same buffer used above was prepared and injected to the measuring chambers as described above. The CNC solution was incubated in the chambers for 3 hours and then washed with same buffer solution. The washing buffer was then exchanged for 50 mM sodium phosphate buffer pH 7 containing 200 mM NaCl to block any binding due to ionic interactions.

Sensograms as bound mass vs. time of the QCM binding studies are shown in Figure S3. The experiment can be divided into three regions, the initial equilibration (baseline), injections of the protein (first vertical line) and CNC (second vertical line). In addition, the surfaces were washed with buffer after each injection. The amount of bound masses were estimated from the frequency change by Sauerbrey equation

$$\Delta m = -\frac{C\Delta f}{n} \quad (\text{Eq S2})$$

where C is a constant $17.7 \text{ ngHz}^{-1}\text{cm}^{-2}$ arising from the properties of the quartz crystal, Δf is the frequency change and n is the overtone of the oscillations. Note that estimation of mass is quantitative for the bound protein, since they form a rigid film having similar acoustic properties with the quartz crystal. This could be verified by measuring the dissipation of the crystal oscillations during binding. Value of dissipation (not shown) remained low for HFBI and HFBI-DCBD layers, less than 0.5 and 2×10^{-6} , respectively, but increased significantly during binding of CNC.

Injecting of HFBI over a PS surface is known to lead to formation of a monomolecular layer of hydrophobin on the surface. This can be seen for the initial parts of the QCM sensograms for both HFBI and the HFBI-DCBD fusion proteins. Mass of bound HFBI was 200 ng/cm^2 and the HFBI-DCBD bound to a level of 650 ng/cm^2 . The bound amounts correspond to mean molecular area of $\sim 6.3 \text{ nm}^2$ for HFBI and $\sim 4.7 \text{ nm}^2$ for HFBI-DCBD. After protein injection and rinsing, a solution of CNC was injected. The Sauerbrey mass of bound CNC on the HFBI layer was 900 ng/cm^2 and the mass bound to HFBI-DCBD was approximately $3.0 \mu\text{g/cm}^2$. Sauerbrey equation is only valid for thin, rigid films, assuming negligible dampening of the oscillations. The measured dissipation (ΔD) values for CNC binding, however, were significant (12 and 30×10^{-6} to HFBI and HFBI-DCBD respectively) and thus their calculated masses are most likely underestimated. The larger the ΔD value, the larger the underestimation is. Nonetheless we can use the Sauerbrey masses as estimations and draw the conclusion that the monolayer of HFBI-DCBD fusion protein has a much higher capability of binding cellulose than wild-type HFBI.

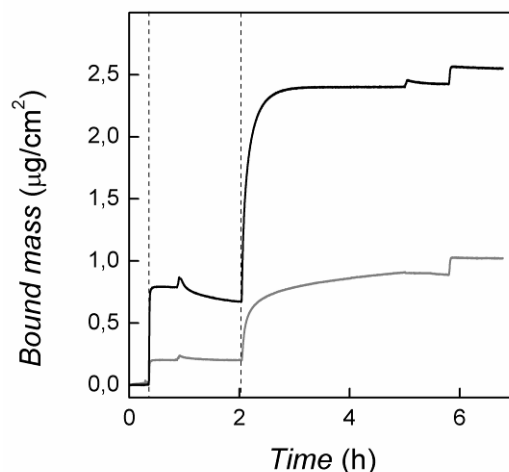


Figure S3. A QCM sensogram of consecutive binding of HFBI (grey line) and HFBI-DCBD (black line) to PS surface and CNC to the resulting protein layers. Injection times of protein and CNC solutions are marked with vertical lines to the image.

Interfacial Shear Rheology

Interfacial shear rheology was measured using TA Instruments AR-G2 controlled stress rheometer equipped with a Du Noüy –ring geometry. The experiments were made on air/water interface at 20 °C. The interfacial films of 0.54 µM HFBI-DCBD with and without nanocellulose were aged in the measuring cup for 20 h. For 1.3 µM HFBI and HFBI-DCBD the interfacial films were not aged before the measurement, instead the evolution of the interfacial film was measured. Rotational and oscillatory mappings were done before each measurement. The ring was carefully placed onto the interface, immersed into the sample and then brought back onto the interface by automatic control of the geometry height. Three different measurement types were performed for the aged interfacial films: A time dependent experiment at constant frequency (0.1 Hz) and strain (0.01 %), a frequency dependent experiment at constant strain (0.01%) and a strain dependent experiment at constant frequency (0.1 Hz). The frequency dependent experiment was done after the time dependent measurement for the same interfacial film, since the films remained stable. The strain in the above experiments was set to 0.2 % to ensure that the experiments were done in the linear viscoelastic regime. The strain value was selected from a strain dependent experiment where strain was varied from 0.001 to 10 % at a constant 0.1 Hz frequency.

Viscoelastic shear moduli resulting from the adsorption of HFBI and HFBI-DCBD as a function of time are shown in Figure S4. In the case of HFBI–DCBD the G' value after three hours is almost an order of magnitude lower compared to HFBI. The HFBI–DCBD film forms slower than the film of HFBI in consistency with the observations done by ellipsometry. The G' of HFBI-DCBD starts to increase 75 minutes after starting the measurement, whereas G' of HFBI starts to evolve after ~ 20 minutes. The high values of rheological moduli for wild type HFBI are most likely due to strong lateral interactions between the molecules. For more bulky HFBI-DCBD, the values are significantly lower because tight packing of the molecules is sterically hindered, lessening the interaction between the HFBI units.

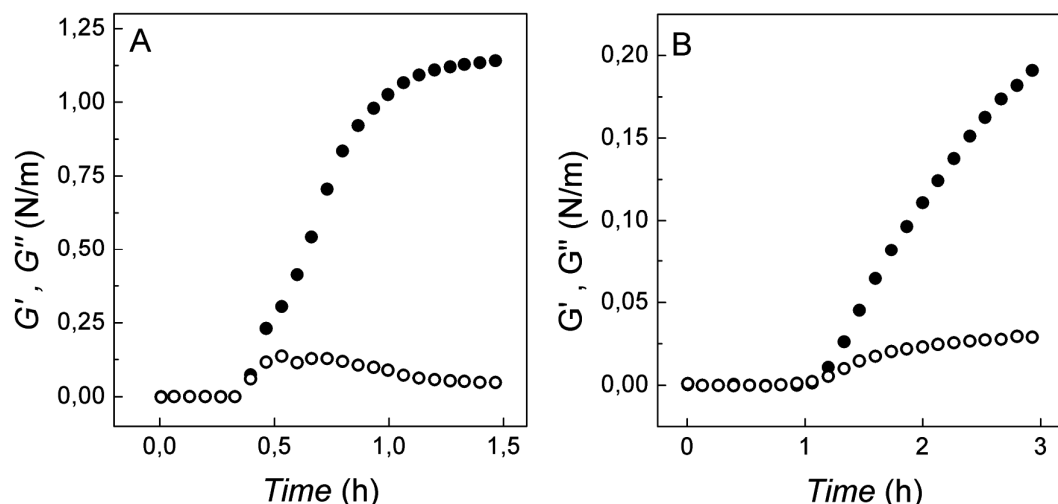


Figure S4. Surface shear moduli of 1.3 μM HFBI (A) and HFBI-DCBD (B) as a function of time. Elastic modulus G' is plotted as the closed circles and viscous modulus G'' as the open circles. Measurements were carried out using constant 0.2 % strain and 0.1 Hz frequency.

Time dependent changes in aged films of 0.54 μM HFBI-DCBD and its mixture with 0.025 mg/ml NFC were studied by exposing them to constant strain and frequency (Figure S5). Addition of NFC to the interface increased the G' values slightly, but the most prominent change was in the increased deviation between parallel experiments done on the NFC containing films. The studied ratio of HFBI-DCBD to NFC represents a situation where ~ 50 % of HFBI-DCBD is associated with NFC; the free HFBI-DCBD concentration being roughly 12 μM and the amount of bound HFBI-DCBD being approximately 5 $\mu\text{mol/g}$ (not fully saturated). Absolute values of the rheological moduli for a hybrid film containing both HFBI-DCBD and NFC does not significantly differ from the values for the film of HFBI-DCBD only. This indicates that the protein forms a stable interfacial layer, which the NFC does not penetrate. However, the deviation of measured curves increases, probably due to variation in the density of NFC fibrils that are attached to the HFBI-DCBD film at the interface.

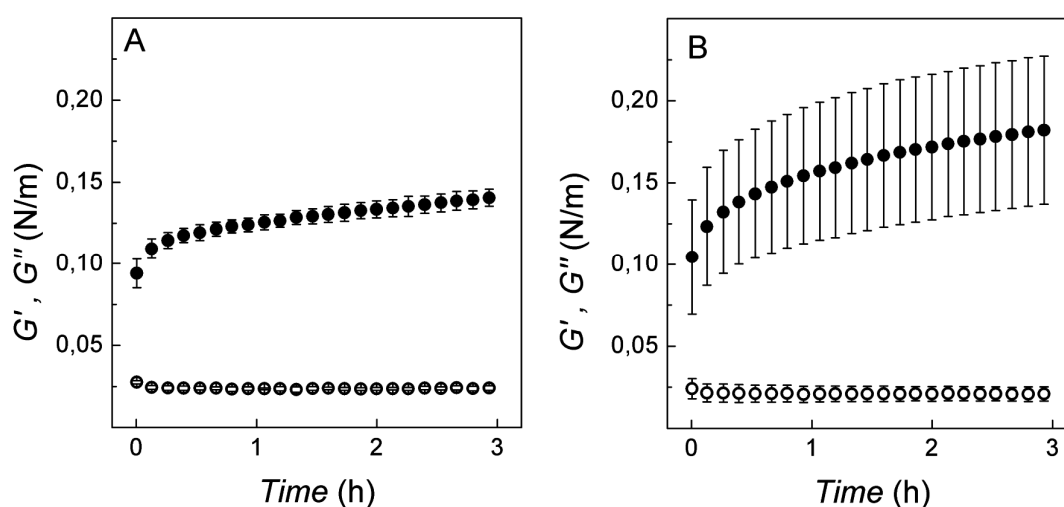


Figure S5. Surface shear moduli of 0.54 μM HFBI-DCBD (A) and 0.54 μM HFBI-DCBD with 0.025 g/l NFC light fraction (B) as a function of time. Elastic modulus G' is plotted as the closed circles and viscous modulus G'' as the open circles. Error bars are calculated from

the standard deviation of 3-5 measurements. Measurements were carried out using constant 0.2 % strain and 0.1 Hz frequency.

In the frequency dependent measurement one can note that the G' value of both film types increased monotonically over the investigated frequency range and interfacial shear viscosity $|\eta^*|$ of both samples decreased (Figure S6). The similar behaviour of the two films under increasing frequency indicates that the NFC does not have a significant effect on the protein film properties. Logarithm of the interfacial viscosity is inversely proportional to the frequency on logarithmic scale and indicates shear thinning behavior. Both interfacial shear viscosity and viscoelastic moduli had a power law dependency on frequency (eg. $G' \propto \omega^n$). Power law constants N , n' and n'' extracted from the slopes of viscosity, G' and G'' on log-log scale are summarized in table S1.

Table S1. Power law constants for HFBI-DCBD and HFBI-DCBD/NFC films.

	HFBI-DCBD	HFBI-DCBD + NFC
N (viscosity)	-0.86	-0.92
n'	0.12	0.12
n''	0.07	0.07

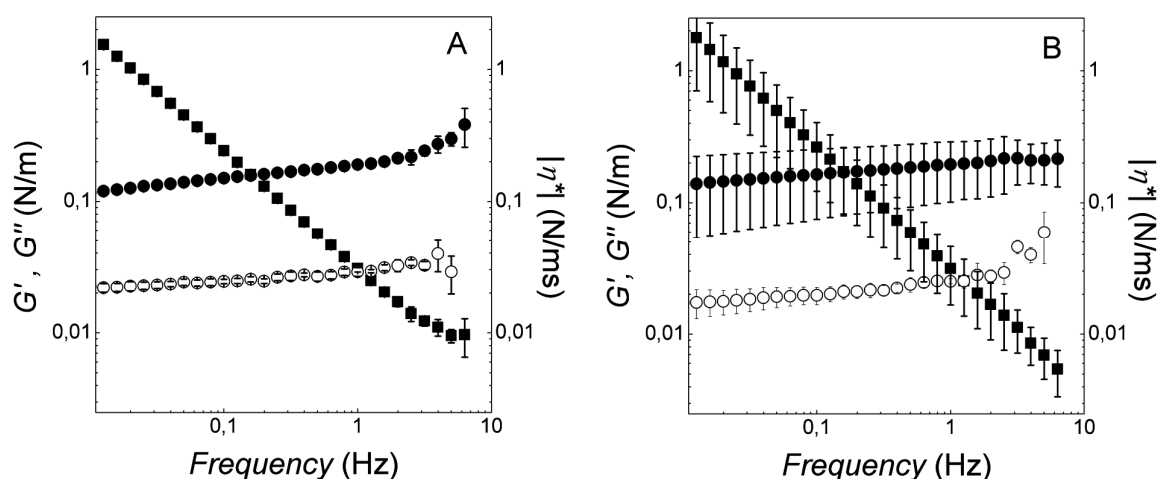


Fig S6. Surface shear moduli and interfacial shear viscosity of 0.54 μM HFBI-DCBD (A) and 0.54 μM HFBI-DCBD with 0.025 mg/ml NFC light fraction (B) as a function of frequency. Elastic modulus G' is plotted as the closed circles, viscous modulus G'' as the open circles and interfacial viscosity as squares. Error bars are calculated from the standard deviation of 3-5 measurements. Measurements were carried out using constant 0.2 % strain. The power law constant of the shear viscosity was -0.86 for HFBI-DCBD and -0.92 for the combination.

In the strain dependent measurements one can see the collapse of the viscoelastic moduli at strain 0.25 % (Figure S7). Absolute values of G' is again higher for the NFC containing film, but similar behaviour of the two films under increasing strain indicates that NFC does not otherwise affect on the interfacial properties of the protein film.

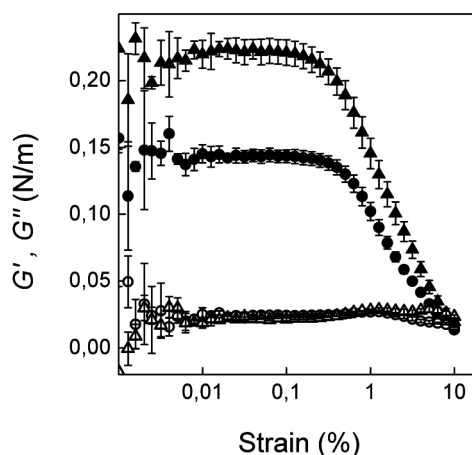


Fig S7. Surface shear moduli of 0.54 μM HFBI–DCBD (circles) and its combination with 0.025 g/l NFC (triangles) as a function of % strain. Elastic modulus G' is plotted as the closed symbols and viscous modulus G'' as the open symbols. Error bars are calculated from the standard deviation of 3-5 measurements. Measurements were carried out using a constant 0.1 Hz frequency.

Emulsification Experiments

Emulsions stabilized with NFC were imaged with optical microscopy. The oil/water interface is clearly visible in bright field images as circular lines (Figure S8A). For verification that an oil-in-water type emulsions were indeed formed, the oil phase was stained with a lipophilic dye (Nile Red) and the emulsion was imaged with a confocal microscopy. In Figure S8B it clearly seen that the droplets were colored and the continuous phase remained unstained. Emulsions stabilized with combinations of NFC, CNC and HFBI-DCBD were imaged similarly and are presented in Figures S9 and S10. The structure of all emulsions appear more or less similar, but the droplet size in emulsions including HFBI-DCBD was much smaller, only hundreds of nanometers (Figure S9). In Figures S9A, S10A and S10C cellulose has been stained with Calcofluor.

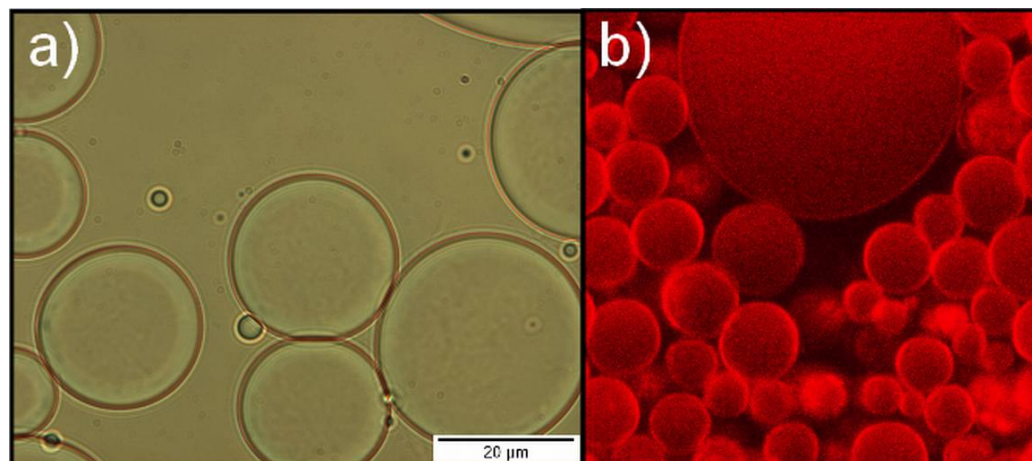


Figure S8. Emulsions stabilized with NFC. A) A bright field microscopy image of emulsion droplets. B) A confocal microscopy image where the oil phase has been stained with Nile Red. Image size is $26 \times 26 \mu\text{m}$.

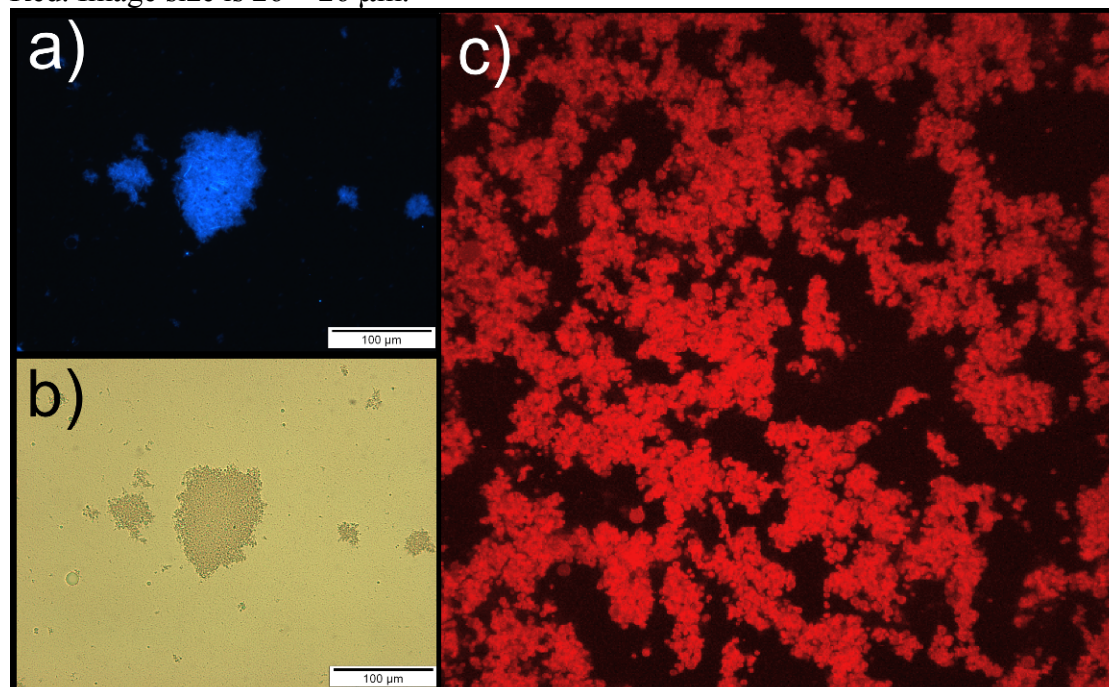


Figure S9. Emulsions stabilized with NFC and HFBI-DCBD. An epifluorescence (A) and a bright field (B) image of emulsion containing nanodroplets associated into larger agglomerates. C) A confocal microscopy image of an emulsion where oil phase has been stained with Nile Red. Image size is $128 \times 128 \mu\text{m}$.

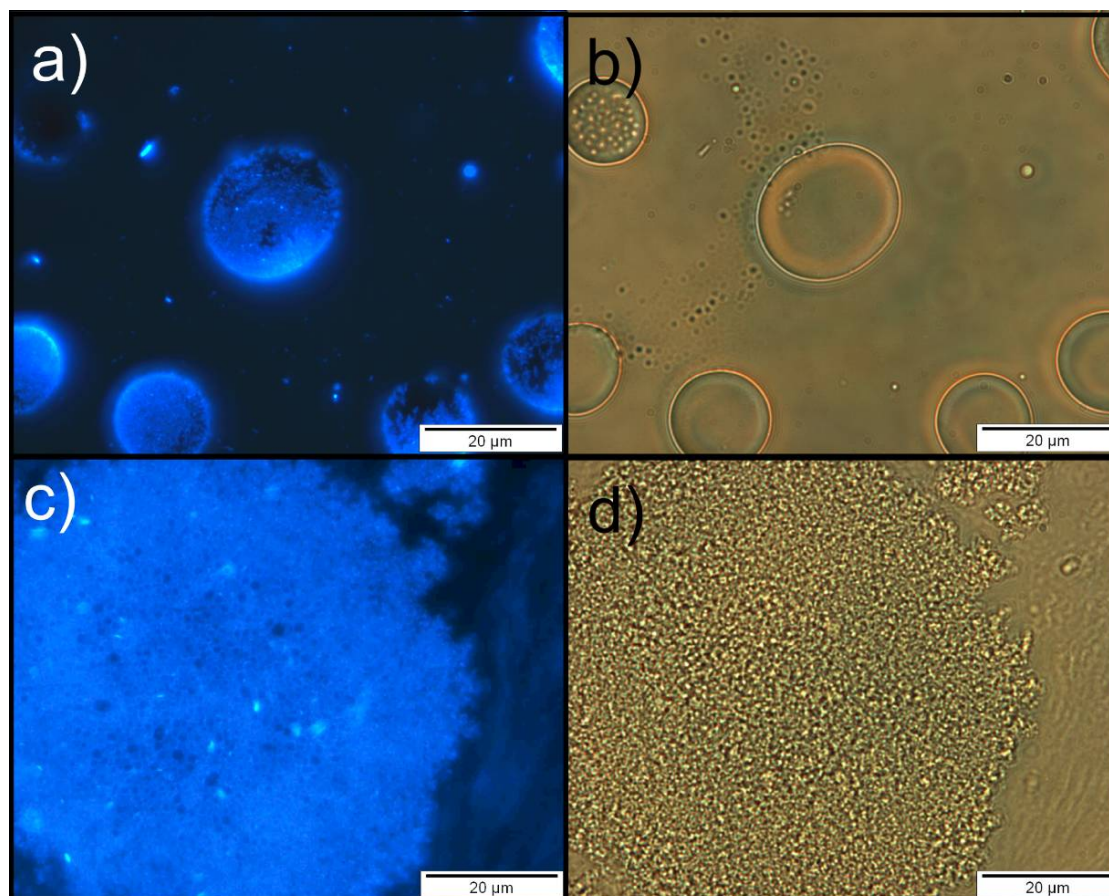


Figure S10. Emulsions stabilized by cellulose nanowhiskers. An epifluorescence (A) and bright field image (B) of an emulsion stabilized by CNC. An epifluorescence (C) and bright field image (D) of an emulsion stabilized by CNC and HFBI-DCBD. Cellulose was stained with Calcofluor.

Stability of emulsions containing only HFBI-DCBD, cellulose nanowhiskers or both in water-hexadecane mixtures was also studied. Emulsion stability indices for these systems are presented in Figure S11. Since hydrophobins are amphiphilic and assemble at oil/water interface, they are also able to stabilize emulsions. In Figure S11A, it is clearly seen that stability of emulsions is increased as the concentration of HFBI-DCBD is increased and reaches a limiting value of about 80 vol-% at concentration 1.5 mg/ml. When cellulose nanowhiskers are added to the system containing 1 mg/ml HFBI-DCBD, a significant decrease in emulsion stability is observed (Figure S11B). However, compared to emulsions stabilized with only CNC, the combination with protein shows better emulsification ability, by increasing the final volume from about 30 % to 50 %.

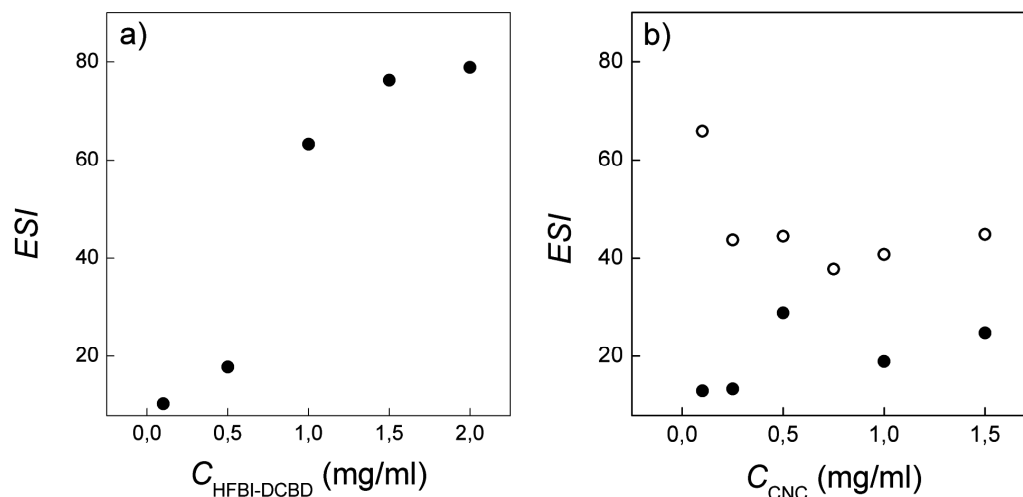


Figure S11. ESI of emulsions stabilized by varying amount of HFBI-DCBD (A), cellulose nanowhiskers (B, black dots) and 1 mg/ml HFBI-DCBD and varying amount of cellulose nanowhiskers (B, open dots).

Binding of Drug Nanoparticles to NFC

For cellulose binding studies, the particles were either prepared with HFBI or HFBI-DCBD coatings. When the nanoparticles were mixed with cellulose, the particles spontaneously attached to the cellulose nanofibrils (Figure S12). This happened with both HFBI and HFBI-DCBD coatings. The lifetime of the particles increased dramatically, and no degradation was observed within 4 weeks. Even though the particles slowly sediment to the bottom of the vial during storage when bound to NFC, they can be readily re-dispersed with no apparent degradation. The particles are not removed even with mechanical activation, e.g. when subjected to concentration, drying and re-dispersion in water.

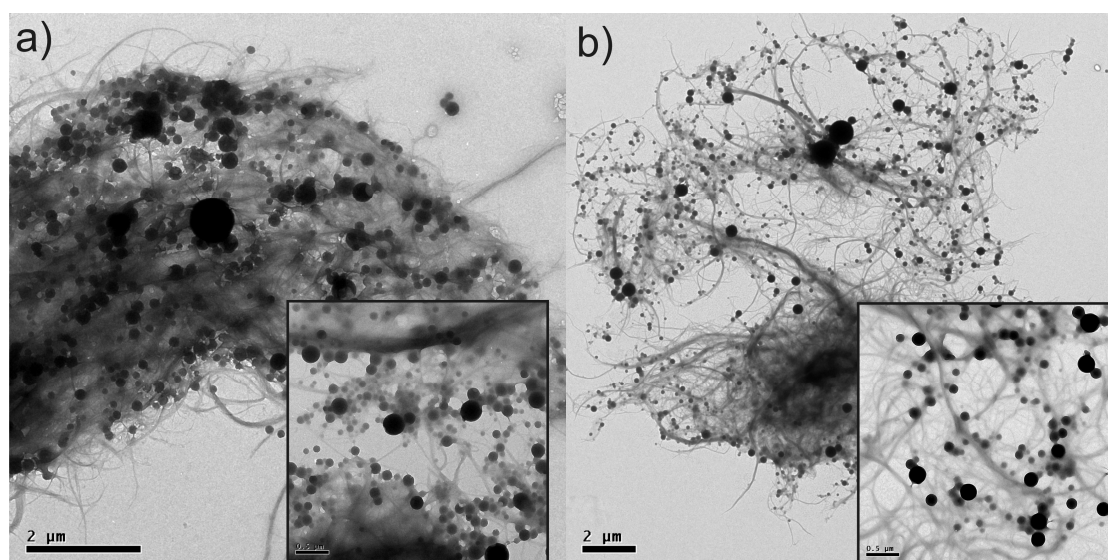


Figure S12. TEM images of a) ITR-HFBI-NFC samples and b) ITR-HFBI-DCBD-NFC samples. Insets show close-ups of the particles.

References

ⁱ Tompkins, H. G., & Irene, E. A. (Eds.), Handbook of ellipsometry (2005) Heidelberg, Springer.

ⁱⁱ de Feijter, J. A., Benjamins, J., & Veer, F. A. Ellipsometry as a Tool to Study the Adsorption Behavior of Synthetic and Biopolymers at the Air-Water Interface, *Biopolymers* (1978) 17, 1759.

ⁱⁱⁱ Ball, V., & Ramsden, J. J. Buffer Dependence of Refractive Index Increments of Protein Solutions. *Biopolymers* (1998) 46 (7) 489.

^{iv} Azzam, R. M., & Bashara, N. M. Ellipsometry and Polarized Light (1977) Amsterdam: North-Holland.